IRANIAN JOURNAL OF PHYSICS RESEARCH

Iranian Journal of Physics Research, Vol. 19, No. 3, 2019

Research note

Designing and developing a photo detector (CdS/Si)

R Aljarrah and A Aljobory
Department of Physics, Faculty of Science, University of Kufa, Najaf, Iraq

(Received 24 February 2018 ; in final form 17 December 2018)

Abstract
Cadmium sulfide (CdS) thin films were prepared using the technique of spray pyrolysis included the glass and Si wafer (300 nm thick) using Cadmium Acetate Cd $(CH_3COO)_2 \cdot 2H_2O$ and Thiourea $(CS(NH_2)_2)$. These compounds are used as the control materials of Cd^{+2} and S^{-2} ions, respectively. The films were annealed at different temperatures (400, 500, and 600°C). The high-quality films were obtained using XRD analysis. X-ray diffraction analysis for all CdS films was polycrystalline with a cubic and hexagonal structure of H (002) and C (111). It is difficult to distinguish between them, after the temperature from 400 °C to 600 °C, new peaks of the hexagonal structure appeared. The maximum value of responsivity occurred at a wavelength of 500 to 560 nm. It has been observed that the best spectral response occurs when the annealing temperature is 500°C. The highest peak have obtained within the wavelengths between 500- 560 nm signifies the greatest response and the greatest quantitative and qualitative detection efficiency as it ranges with an annealing temperature.

Keywords: Responsivity, Spray pyrolysis, Hexagonal wurtzite, Quantum efficiency, Specific detective

1. Introduction
Cadmium Sulfide (CdS) is a well-known group II-VI semiconductor and favorable material for electronic and optoelectronic implementations. CdS film has been of interest because of rising photoconductivity in the visible area, high absorption coefficient, high electron affinity, easy ohmic contact, and little resistivity [1, 2]. It has the direct gap energy of 2.42 eV at 27°C. CdS is used in several devices: transistor, photo sensors, gas sensors, light emitting diodes, logic circuits [3-8] and optoelectronic devices, particularly photodetectors, and solar cells. It occurs naturally as an n-type semiconductor. This behavior of CdS comes from sulfur vacancies (VS) and cadmium interstitials (Cdi) [9]. There are different physical and chemical ways to prepare CdS. The spray pyrolysis technique was found for CdS thin film deposition. This technique is relatively easy to scale up for large-area deposition [10, 11]. The reason for using CdS is due to providing a chemical solution. It is simple to provide the CdS as a thin film with good quality at room temperature. The present study was addressed to investigate the annealing temperatures effect on the CdS film structure and to find the optimum condition for CdS thin films as a photoconductive device by using CdS/p-Si photovoltaic. A photoconductor consists simply of a slab of semiconductor with ohmic contacts at both ends of the slab (Figure 1). When incident light falls on the surface of the photoconductor, electron-hole pairs are generated either by band-to-band transition (intrinsic) or by transitions involving forbidden-gap energy levels (extrinsic), resulting in an increase in conductivity.

2. Materials and Methods
CdS was produced using the aqueous solution of 0.1 M from 6.663 g and 1.903 g of $Cd(CH_3COO)_2 \cdot 2H_2O$ and $CS(NH_2)_2$, respectively, in 250 ml of distilled water for each one; this was done with continuous stirring for 10 minutes using an electronic balance (HR-200 A&D Co.) and a magnetic-stirrer (IKA® C-MAG HS 7). Then an appropriate volume for each experiment was taken, depending on the percentage solution. For instance, Cd:S (0.5:0.5) represented the variation of Cd/S. These materials were used to prepare the solutions deposited on the glass and Si wafer at 400°C. The spray rate of the solution was one sprinkling in a minute; the sprinkling time was 11 s. The distance between the spray nozzle and the substrate was 30 cm. Pure CdS thin films were deposited on glass and Si substrates by the chemical spray pyrolysis technique. Figure 2 shows the spray system used in this work. The substrate temperature was maintained to be ~350°C during spraying with ±10°C. To avoid the excessive cooling of the substrate, spraying was achieved in periods of about 12 sec followed by ~2 mins wait, with the air flow rate of 5 ml/hour . In order to deposit the thin films with uniform thickness, the distance between the substrate and the spray nozzle was kept at 30 cm. After the completion of the spray process, the films were annealed at (400, 500 and 600°C) for 1 hour by using the CARBOLITE (CWF 1200) device. The film's thickness (t) was determined using the weighing-method.

$$t = \frac{\Delta m}{A\rho} v, \tag{1}$$

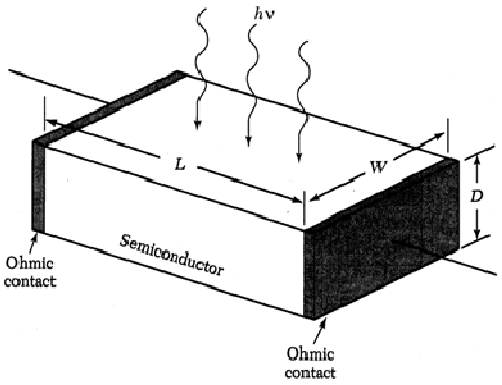

Figure 1. Schematic diagram of a photoconductor consisting of a slab of semiconductor and two contacts at the ends.

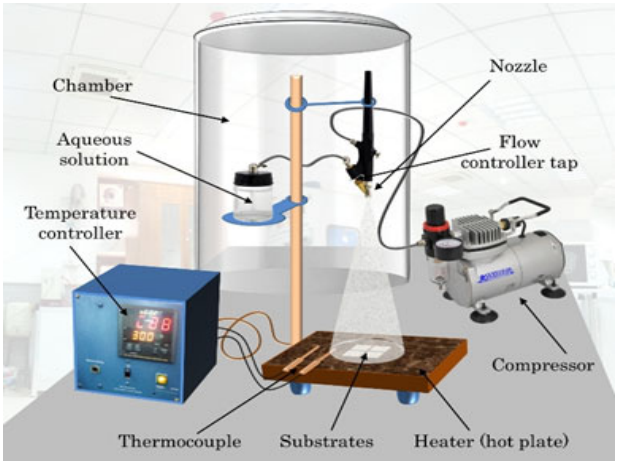

Figure 2. (color online) Spray pyrolysis system.

where Δm= the mass difference of slide, A= the area of 2.5×2.5 cm^2, and ρ= CdS the density of 4.824 g cm^{-3}. The CdS structure was examined using X-ray diffraction by an X-ray diffractometer system of λ = 1.5406Å. The corresponding inter planer spacing (d_{hkl} Å) was calculated using the Bragg's law:

$$2d \sin\theta = n\lambda \,, \tag{2}$$

where d = the perpendicular distance between two the pairs of the panels in the crystal. The average crystallite size was calculated by the Scherer's formula:

$$D = \frac{0.9\lambda}{\beta\cos\theta}, \tag{3}$$

where D is the average crystallite size (nm) and β is the full-width half-maximum intensity (degs.). Photodetector characteristics (quantum efficiency, and signal to noise ratio, equivalent noise power, and detective) of CdS/Si were measured. These were monochromatic in the range of 200-900 nm.

3. Results and discussion

Figure 3 shows the X-ray diffraction of CdS with different temperatures (400, 500 and 600ºC). CdS had the mixtures of cubic and hexagonal structures. It was difficult to distinguish between cubic (111) and HCP (002), as well as cubic (220) and HCP (110). New peaks of hexagonal structure appeared at the X-ray diffraction. This phenomenon was thought to be the phase change of CdS using the heat treatment. The hexagonal mixtures and cubic phase were changed to the hexagonal phase by the heat treatment because the hexagonal phase of CdS was more thermodynamically stable than the cubic phase of CdS [12]. The XRD patterns revealed that highest peaks corresponded to the H (0 0 2) C (111), (220), and (103). It also showed a hexagonal (100), H (110), C (220), and C (311) [13]. The corresponding values of the inter planar spacing "d" were calculated and compared with the standard values of the JCPDS data. The annealing resulted in the good quality of films with improved crystallinity, as evidenced by diffraction peaks; the first X-ray diffraction appeared at the annealing temperature of 500ºC. The FWHMs for all peaks and crystallite size (G.S) were measured. The crystallite size (D) was increased with annealing, indicating the agreement with the grain growth of CdS [13].

The spectral responsivity of the detector was measured. The responsivity for monochromatic light wavelength is given:

$$R_\lambda = \frac{I_{\text{ph}}}{P_{\text{in}}} \quad \text{or} \quad R_\lambda = \frac{V}{P_{\text{in}}}, \tag{4}$$

Figure 4 and table 1 show the wavelength-dependence of the spectral responsivity (R_λ) for CdS/Si heterojunction at 10 V for different temperatures. The maximum photo responsivity was peaked at about 500-560 nm. The optoelectronic characteristics showed that CdS/Si had good responsivity in the visible and near infrared spectra because of the short circuit formatted by the Si substrate. CdS is a window for visible radiation. The cut-off at a wavelength of 500 nm agreed with the CdS energy band gap of 2.4 eV. The responsivity was decreased at the higher wavelength due to the decrease in the penetrating light and the increase of the surface recombination. When the annealing temperature was raised, the spectral responsivity value was raised. The best responsivity was obtained at 500ºC; then the spectral responsivity decreased gradually. This could be attributed to the increasing roughness with the rise of annealing temperature, which enhanced absorption coefficient. Then more power of the incident radiation is absorbed by film,

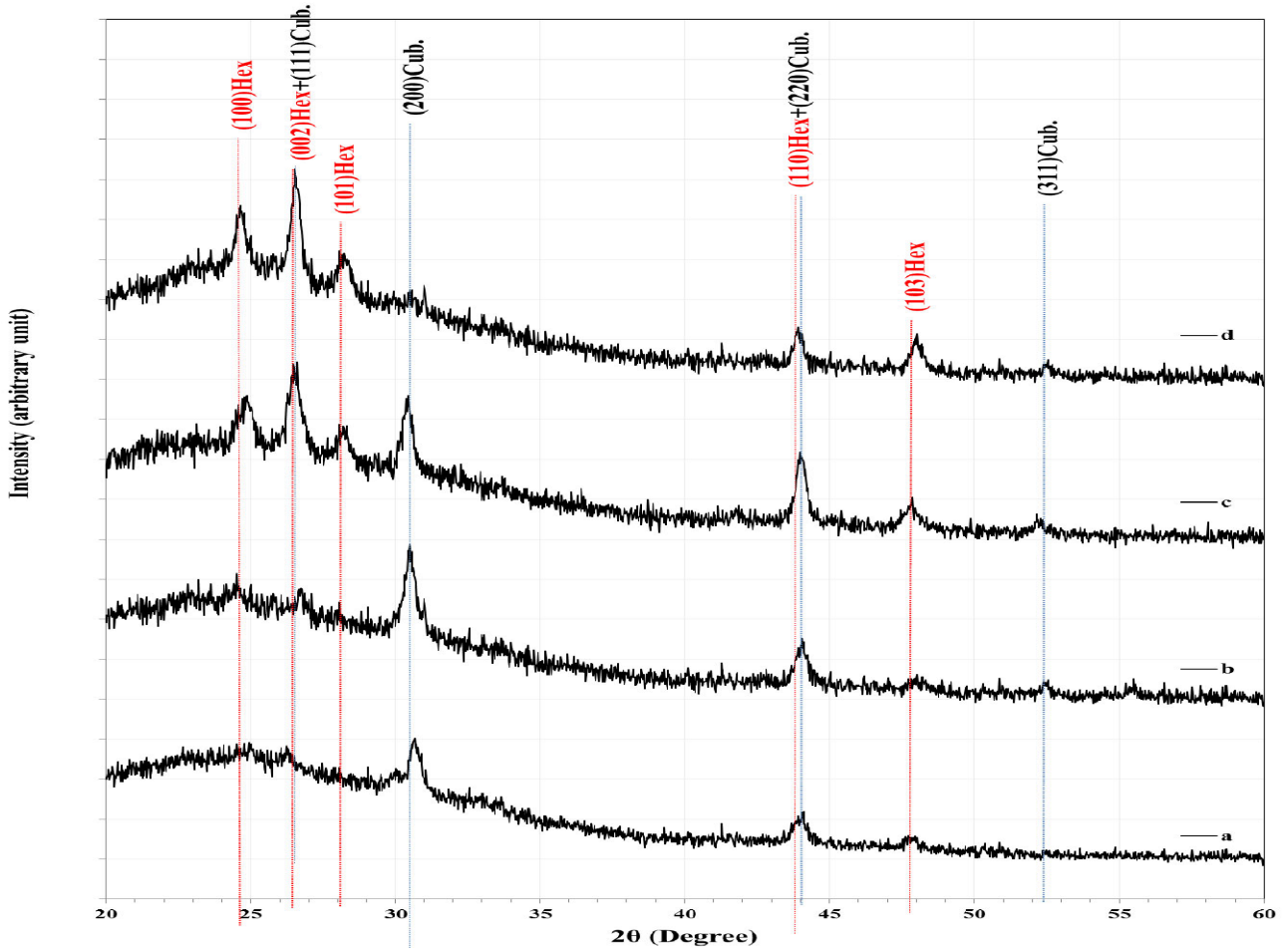

Figure 3. (color online) XRD for CdS at different temperatures (a) *R. T*, (b) 400ºC, (c) 500ºC, and (d) 600ºC.

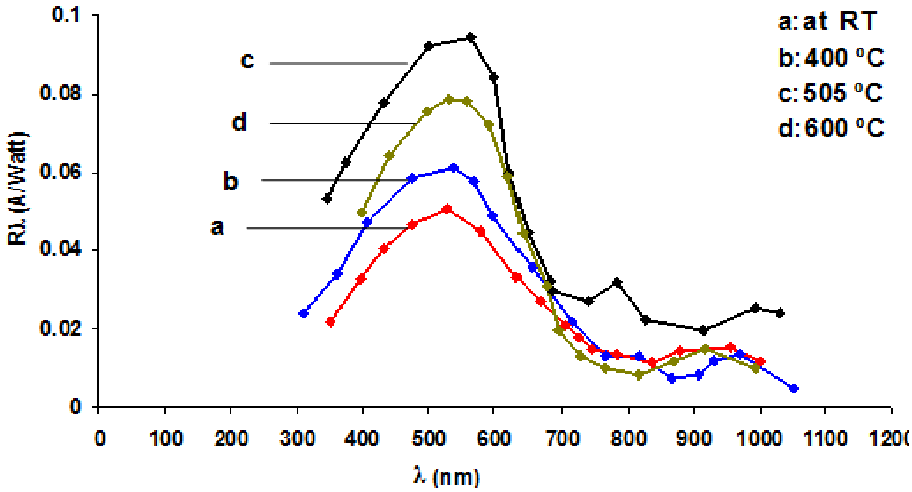

Figure 4 (color online) The variation of spectral responsivity as a function of λ for CdS/Si.

Table 1. CdS/Si detectors with different T_a.

T_a (°C)	λ_{peak} (nm)	R_λ (Amp/W)	η%	NEP×10^{-11} (Watt)	D×10^{10} (cm.Hz$^{1/2}$.W^{-1})	D^*×10^{10} (cm.Hz$^{1/2}$.W^{-1})
RT	560	0.054	12.2	23.1	0.515	0.325
400	540	0.061	14.9	18.5	0.696	0.411
500	500	0.092	24.1	5.6	1.630	1.030
600	510	0.080	19.5	13.2	0.896	0.530

generating electron-hole pairs. Also, the decrease of the responsivity at 600ºC could be increased in the series resistance at the large value of annealing temperature, which tends to decrease the photocurrent.

The peaks of R_λ are shifted to the higher wavelength as T_a was increased due to the decrease of the optical energy gap. The annealing process of the CdS improved the surface roughness and the growth for the buffer layer was optimized to have the best

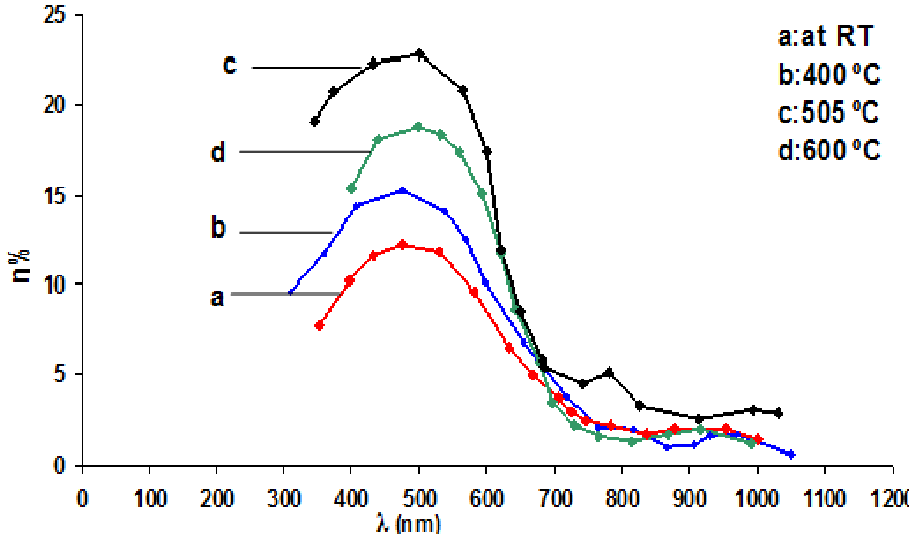

Figure 5. (color online) Efficiency as a function of λ for CdS/Si heterojunction.

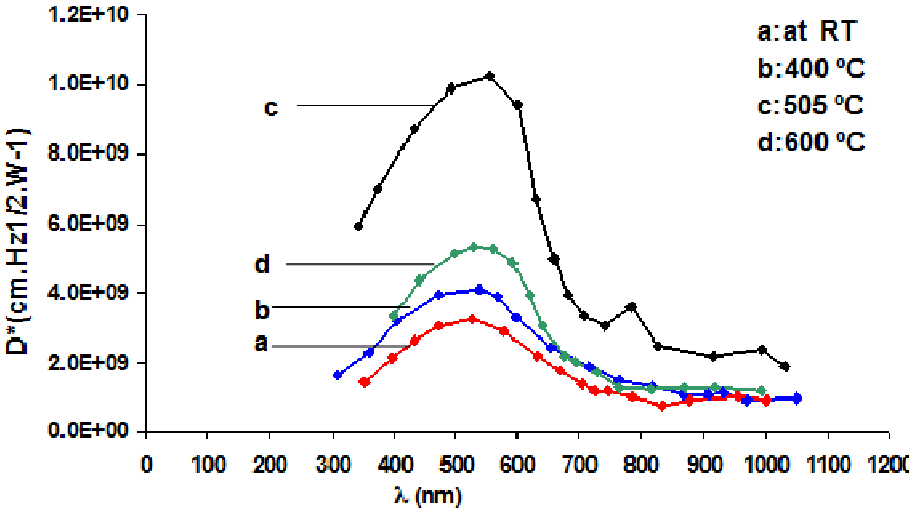

Figure 6. (color online) Specific directivity as a function of λ for CdS/Si.

characteristics at 500°C. The efficiency (η) is important in the photoconductive device, which is recognized by the optoelectronics. It is defined as the ratio of the number of generated electrons in the heterojunction to the that of incident photons on the effective area of the heterojunction. So, η is related to the change of the spectral responsivity according to the relation:

$$\eta = \left(I_{\text{ph}} / \text{e}\right)(h\upsilon / p_{\text{in}}), \tag{5}$$

$$\eta = R_{\lambda}\left(h\upsilon / \lambda e\right), \tag{6}$$

The efficiency was determined as a function of the wavelength for CdS/Si, as shown in figure 6. The quantum efficiency was achieved at 500 nm of 12.2% at *RT* and increased to 24.1% at 500°C and then reduced to 19.5 at 600°C. The reasons are mentioned earlier in the discussion of the spectral responsivity, as shown in table 1.

The Noise-Equivalent Power (NEP) is a concept used to quantify the sensitivity of a detector or the power generated by a source of noise on a detector NEP, which is defined as:

$$\text{NEP} = I_n / R_{\lambda}\left(\text{Watt}\right), \tag{7}$$

The variation of NEP for CdS at different temperatures is shown in table 2. The minimum NEP occurs when RL has the maximum value. NEP decreases with increasing the annealing temperature. This can be attributed to the annealing process of the CdS layer, improving the surface roughness and reducing the recombination process. The specific detective (D^*), which is sometimes called the normalized directivity, is the reciprocal of the Noise-Equivalent Power (NEP) normalized to the detector area of 1.0 cm^2 and a noise electrical bandwidth (Δf) of 1.0 Hz , which is defined as:

$$D^* = D\left(A\,\Delta F\right)^{1/2}, \tag{8}$$

or

$$D^* = R_{\lambda}\left(A\,\Delta F\right)^{1/2} / I_{\text{n}}, \tag{9}$$

D^* was measured as a function of the light wavelength at different temperatures. When the annealing temperatures were raised, then the D^* could increase. These increases in D^* values could be due to the decrease of NEP. D^* increased with raising T_a until 500^0C; then it was decreased with increasing T_a; it was reduced to be about half value when temperatures varied from 500 to 600°C due to increasing the recombination centers, which is due to the effect on D^*.

The response time of the fabricated CdS was tested with the nitrogen laser of 0.3 ns and the energy of 50 μj. It was noticed from the pulse shape that the rise time was 170 μs and the fall time was about 750 μs. The slow decay time was due to the slow escape of holes from the tarps. The hole was captured by the traps that might be emitted back into the valence band according to a time constant depending on the energy between the corresponding hole traps and the edge of the valence band.

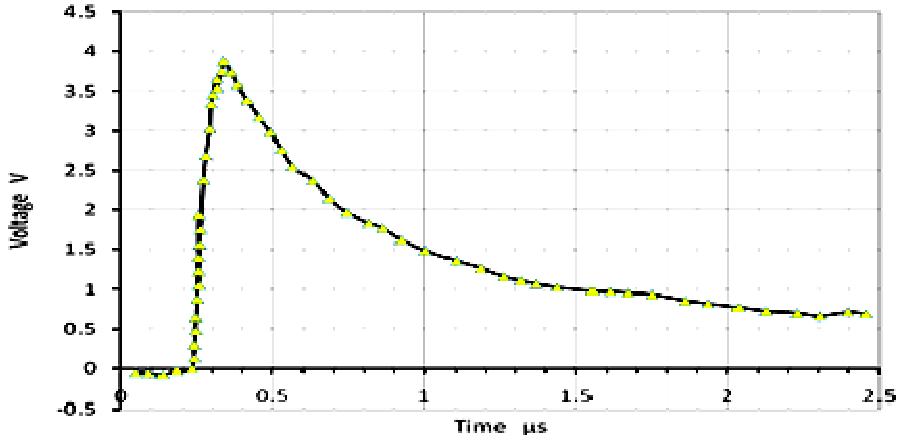

Figure 7. (color online) Photo response time of CdS/Si

The deep traps had a slow response and a slow fall time of the output pulse (figure 7). The long tail accompanying the pulse was due to heating the sample by the high repetitions rate of the N2 laser [14].

4. Conclusions

X-ray diffraction results showed the phase change of CdS from cubic structure to a hexagonal wurtzite one through annealing process and the improvement of crystallization. In this study, the best composition of CdS was at T_a=500°C. The response time, specific detective, and efficiency were increased and shifted to higher wavelengths with increasing T_a. The maximum quantum efficiency was about 24.1 and the particular detective was (1.03 cm. Hz)$^{1/2}$ at 500°C. Overall, the optimum annealing temperature of the CdS/Si photodetector was 500°C.

5. Acknowledgement

The authors acknowledge the financial support of the Kufa University, Iraq. The authors are also grateful to Dr. Basim A Almayahi, Department of Environment, College of Science, University of Kufa, for assisting us throughout this present research.

References

1. J H Lee, *J. Electro.* **17** (2006) 1103.
2. A Ileperuma, C Vithana, K Premaratne, S N Akuranthilaka, S M McGregor, and I M Dharmadasa, *J. Mate. Sci.* **9** (1998) 367.
3. A Palafox, G Romero-Paredes, A Maldonado, R Asomoza, D R Acosta, and J Palacios-Gomez, *Solar Enr. Mat. Solar Cells.* **55** (1998) 31.
4. W Wondmagegn, I Mejia, A Salas-Villasenor, H J Stiegler, M A Quevedo-Lopez, R J Pieper, and B E Gnade, *Micro. Engi.* **157** (2016) 64.
5. B G An, Y W Chang, H R Kim, G Lee, M J Kang, J K Park, and J C Pyun, *Sen. Actu.* B: *Chem.* **221** (2015) 884.
6. H H Afify and I K Battisha, *J. Mat. Sci. Mat. Elect.* **11** (2000) 373.
7. A K Bansal, F Antolini, S Zhang, L Stroea, L Ortolani, M Lanzi, and I D W Samuel, *J. Phys. Chem.* C **120** (2016) 1871.
8. R M Ma, L Dai, H B Huo, W J Xu, and G G Qin, *Nano Let.* **7** (2007) 3300.
9. F Gemain, I C Robin, S Renet, and S Bernardi, *Physica Status Solidi* **9** (2012) 1740.
10. J Hernández-Borja, Y V Vorobiev, and R Ramírez-Bon, *Solar En. Mater. Solar Cells* **95** (2011) 1882.
11. M Bedir, M Öztaş, and H Kara, *J. Mat. Sci.* **24** (2013) 499.
12. P N Gibson, M E Özsan, D Lincot, P Cowache, and D Summa, *Thin Solid Films* **361** (2000) 34.
13. H El Maliki, J C Bernede, S Marsillac, J Pinel, X Castel, and J Pouzet, *App. Surf. Sci*. **205** (2003) 65.
14. A M Suhail, E K Hassan, S S Ahmed, and M K M Alnoori, *J. Elect. Dev.* **8** (2010) 268.